Acta Cryst. (1996). B52, 596–604

A Critical Review of the Experimental Valence Charge Density of GaAs

ULLRICH PIETSCH[a]* AND NIELS K. HANSEN[b]

[a]*Institut für Festkörperphysik der Universität Potsdam, D 14415 Potsdam, Germany, and* [b]*Laboratoire de Cristallographie, Faculté des Sciences, Université de Nancy, F 54506 Vandoeuvre-les-Nancy Cedex, France. E-mail: upietsch@persius.rz.uni-potsdam.de*

(*Received 4 December 1995; accepted 11 March 1996*)

Abstract

The valence charge and difference densities of GaAs have been calculated without previous refinements of a charge density model using six different data sets of X-ray structure amplitudes published until now. Since the data sets have been measured by means of different experimental methods and due to the different data treatment, the individual structure factors differ on the absolute scale. Furthermore, different temperature factors have been published. In order to bring the data to a common level, we used the same two harmonic temperature factors and the same algorithm for correcting the different sets of experimental data for anomalous dispersion. Because of the non-centrosymmetry of the zinc blende structure, these procedures are not strictly model-independent. A simple bond charge model was used to obtain phases of the structure amplitudes and to perform the above-mentioned corrections. In general, the details of 'experimental' charge densities depend sensitively on the balanced ratio among the structure factor moduli used. A smooth density map is only obtained if all F have the same high level of accuracy [$\delta(F)/F \leq 1\%$] and if 'outliers' are omitted. Only four of the six data sets describe the covalent bond and the partial charge transfer between neighboring atoms, in qualitative agreement with our expectation based on the results of pseudo-potential calculations. However, some quantitative discrepancies remain, particularly in the height of the charge density maximum between nearest neighbours and in some details outside the bonding region.

1. Introduction

The major problem in comparing experimental and theoretical electron densities is that a truly experimental charge density does not exist. One reason for this is that a measurement of Bragg intensities only leads to moduli of the X-ray structure factors which contain not only the Fourier transform of the charge density, but also for heavier atom structures a contribution from anomalous scattering. This contribution of anomalous dispersion to the structure factor (a complex number) can only be calculated if the positions and the thermal parameters of the atoms within the unit cell are known. For non-centrosymmetric structures, where the structure factor has a phase which we do not know, this correction cannot easily be subtracted. We therefore need a model for the electron density in order to obtain a phase of the total structure factor. The model should contain as small a number of parameters as possible in order to minimize the influence of preconceived ideas on the final results.

In the present article we are concerned with the study of the electron density distribution in GaAs (space group $F\bar{4}3m$), which has been investigated by DeMarco & Weiss (1964) for the first time. They found a significant increase of the (200) scattering power. It was simply explained by an ionic charge transfer and led to the definition of an effective ionic charge by Attard (1968). As found by Cole & Stemple (1972) for the (111) and by Colella (1971) for the (222) Friedel pairs, the integral intensities of hhh and $\bar{h}\bar{h}\bar{h}$ reflections differ much more than owing to the influence of dispersion. This is an indication of the existence of a mixed covalent–ionic bond in GaAs. Bilderback (1975) and Pietsch (1981) have measured additional weak intensity reflections and explained them using a multipole, respectively, a bond charge model, and they obtained a better description of the charge accumulation between nearest neighbours.

A number of theoretical studies have been carried out, giving a good idea how the electron density of GaAs should look. The main feature is a concentration of electrons between next-neighbour atoms that is polarized towards the arsenic. We believe that this feature really exists and use it as a constraint in our modelling. We would like to verify, by experiment, the position and size of this feature.

With this in mind we compare six data sets, which have been measured using different techniques and under different experimental conditions, but all at room temperature:

Matsushita & Hayashi (1977) measured ten structure amplitudes from the angular width of the respective rocking curves using λ = 1.54 Å. Together with the five weak reflections measured by Pietsch (1981) with the same wavelength, these data were employed to construct the experimental valence charge density of GaAs

(Pietsch, Tsirelson & Ozerov, 1986). Compared with density maps calculated from pseudo-potential methods, the valence charge density verified the existence of a mixed covalent–ionic bond, but it was inaccurate outside the bonding region. The discrepancies have been explained by the limited data set and inaccurate temperature factors.

Since then further data sets have been published. Kobayashi, Takama & Sato (1988) determined 14 $|F|$ of strong reflections measuring the pendellösung fringes from a single crystalline plate using an energy dispersive set-up. A final data set has been published for a wavelength of $\lambda = 0.25$ Å. Due to the small wavelength the data are practically unaffected by anomalous dispersion. Other data sets were collected using standard techniques of crystal structure analysis. Uno, Okano & Yukino (1970) have presented 12 reflections, including the weak 200 reflection. They were measured from a fine crystal powder using copper radiation. These data fulfil the kinematical limit and should be free of secondary extinction. Levalois & Allais (1986) have measured 63 reflections, both weak and strong, from a small single crystalline plate using Ag $K\alpha$ radiation. The data were corrected for extinction and interpreted using a bond charge model. Their model charge density reproduces qualitatively the theoretical charge density of Chelikowski & Cohen (1976). Saravanan, Mohanlal & Chandrasekaran (1992) measured an extended data set with Mo $K\alpha$ radiation in order to determine the anharmonicity of lattice vibrations. Unfortunately, the published weak $|F|$ deviate up to 100% from the theoretical predictions. The refined anharmonic temperature factors are two orders of magnitudes larger than known from other covalently bonded materials (Roberto, Batterman & Keating, 1974). Finally, Stevenson (1994) recently published an extended data set using $\lambda = 0.71$ Å in order to determine the anharmonic temperature factors. After correction of extinction and thermal diffuse scattering, the refined anharmonicity parameter coincides with the value obtained independently by Pietsch, Paschke & Eichhorn (1993, 1994).

The first problem we face is how to compare the data sets. For the correction of anomalous dispersion we need to know the Debye–Waller factor and we use a bond charge model to take into account the above addressed constraint on the charge density. This treatment is applied to all the data sets, the details of which are presented in §2 followed by a comparison of the resulting structure factor moduli.

In §3 and §4 we discuss charge density maps calculated from the various experimental data sets. Based on the criteria given above, we select the data set which we estimate to be the most accurate. It is compared with theoretical calculations.

In conclusion it is discussed how we may improve and complement the best data set in order to reduce the remaining discrepancies between theory and experiment.

2. Data reduction

The GaAs unit cell contains four Ga and four As atoms. They occupy two *fcc* sublattices localized at (0,0,0) and $(\frac{1}{4},\frac{1}{4},\frac{1}{4})$. Using Dawson's (1967) generalized formalism there are four different classes of structure amplitudes. Neglecting anharmonicity, the strong reflections ($h + k + l = 4n$, $n = 1, 2...$) are given by the sum of both sublattices

$$F_s = 4\{(f_{Ga} + f'_{Ga})T_{Ga} + (f_{As} + f'_{As})T_{As}\} + i4\{f''_{Ga}T_{Ga} + f''_{As}T_{As}\}. \quad (1a)$$

The class of weak reflections ($h + k + l = 4n + 2$) is determined by their difference

$$F_w = 4\{(f_{Ga} + f'_{Ga})T_{Ga} - (f_{As} + f'_{As})T_{As}\} + i4\{f''_{Ga}T_{Ga} - f''_{As}T_{As}\}. \quad (1b)$$

The medium reflections are given by

$$F_m = 4\{(f_{Ga} + f'_{Ga})T_{Ga} - f''_{As}T_{As}\} + i4\{f''_{Ga}T_{Ga} + (f_{As} + f'_{As})T_{As}\} \quad (1c)$$

if $h + k + l = 4n + 1$ and

$$F_m = 4\{(f_{Ga} + f'_{Ga})T_{Ga} + f''_{As}T_{As}\} + i4\{f''_{Ga}T_{Ga} - (f_{As} + f'_{As})T_{As}\}, \quad (1d)$$

if $h + k + l = 4n + 3$, where f_i are the atomic scattering factors, and f'_i and f''_i are the real and imaginary parts of the anomalous dispersion correction. f_i decrease with increasing scattering angle θ, whereas the dispersion correction is approximately constant, but depends on the wavelength λ. T_i represent the Debye–Waller factors given by

$$T_i = \exp(-B_i(\sin\theta/\lambda)^2) = \exp(-8\pi^2(\sin\theta/\lambda)^2 kT/\alpha_i). \quad (2)$$

Here, B_i are the harmonic temperature parameters which are inversely proportional to the harmonic force constant α_i using the approximation that the atoms oscillate independently from each other within parabolic potentials (Willis & Pryor, 1975). kT in (2) describes the thermal energy (k is Boltzmann's constant, T is the absolute temperature). Due to the chemical bond the charge density is redistributed relative to the model of independent spherical atoms. Assuming a predominant covalency of the chemical bond, the charge density piles up between next neighbours along the <111> directions of the unit cell. Because of the non-centrosymmetry of the structure and the influence of anomalous dispersion, hkl and $\bar{h}\bar{k}\bar{l}$ reflections are modified differently. In the literature the charge density distribution is frequently

described by either a multipole expansion (Stewart, 1976; Hansen & Coppens, 1978) or a bond charge model (Pietsch, 1981; Levalois & Allais, 1986). Using the latter, a bond charge term BC must be added to the $F(hkl)$ calculated by (1*a*)–(1*d*)

$$\mathcal{F}_{s,w,m} = F_{s,w,m} + BC_{\text{real}} + iBC_{\text{imag}}. \quad (3)$$

Both the real and imaginary parts of the bond charge, BC_{real} and BC_{imag}, decrease very rapidly for increasing $\sin\theta/\lambda$. As shown by Pietsch (1981), the BC scattering factor can be approximated by a simple Gaussian which tends to zero close to $\sin\theta/\lambda \simeq 0.5$ Å^{-1}.

The bond charge model is applied to correct the experimental structure amplitudes $|F_{\text{exp}}|$ for anomalous dispersion. It is better suited than the model of spherical atoms, especially for weak and medium intensity reflections at small $\sin\theta/\lambda$. If the BC site is close to (1/8,1/8,1/8) of the unit cell, strong and weak reflections, with $h^*k^*l = 0$ are not affected by the BC ($BC_{\text{real}} \simeq BC_{\text{imag}} \simeq 0$). In this case there is a definite way to correct the experimental data using equations (1*a*) and (1*b*). We find the reduced amounts $|F_{s0}|$ and $|F_{w0}|$ to be

$$|F_{s0}| = \{|F_{\text{exp}}|^2 - 16(f''_{\text{Ga}}T_{\text{Ga}} \pm f''_{\text{As}}T_{\text{As}})^2\}^{1/2} - 4(f'_{\text{Ga}}T_{\text{Ga}} \pm f'_{\text{As}}T_{\text{As}}). \quad (4a)$$

The positive sign applies to the strong reflections, the negative to the weak. The structure factor phases are generally

$$\varphi_{s0,w0} = 0. \quad (4b)$$

In the case of $h^*k^*l \neq 0$ strong and weak reflections can be corrected if both intensities of Friedel pairs [$F^+ = F_{\text{exp}}(hkl)$ and $F^- = F_{\text{exp}}(\bar{h}\bar{k}\bar{l})$] are measured. Because the influence of the BC on F_s is very small, they may be corrected similar to (4*a*) and (4*b*). In the following we focused on the correction of F_w. The difference between F^+ and F^- is determined by the influence of BC_{imag}, because BC_{real} is small (Pietsch, 1981) and may be neglected. BC_{imag} contributes with positive or negative sign to the imaginary part of F_w. and is obtained from

$$BC_{\text{imag}} = [|F^+|^2 - |F^-|^2]/[16\{f''_{\text{Ga}}T_{\text{Ga}} - f''_{\text{As}}T_{\text{As}}\}]. \quad (5a)$$

The real part F_{real} of the corrected value F_{w0} is given by

$$F_{\text{real}} = \{|F^+_{\text{exp}}|^2 - 16(f''_{\text{Ga}}T_{\text{Ga}} - f''_{\text{As}}T_{\text{As}}) + BC^2_{\text{imag}}\}^{1/2} - 4\{f'_{\text{Ga}}T_{\text{Ga}} - f'_{\text{As}}T_{\text{As}}\}. \quad (5b)$$

Under the assumption that the imaginary part of F_{w0} is solely given by BC_{imag}, the structure factor phase φ_w is obtained by

$$\varphi_w = \arctan(BC_{\text{imag}}/F_{\text{real}}). \quad (5c)$$

Finally, the reduced modulus $|F_{w0}|$ follows from (5*a*) and (5*b*)

$$|F_{w0}| = \{F^2_{\text{real}} + BC^2_{\text{imag}}\}^{1/2}. \quad (5d)$$

Unfortunately, there is no way to correct $|F_{\text{exp}}|$ of the medium intensity reflections. Both BC_{real} and BC_{imag} affect F_m in (3). Therefore, we use a very crude approximation, which is exact for a superposition of independent free atoms

$$|F_{w0}| = G|F_{\text{exp}}|, \quad (6a)$$

with

$$G = (16(f_{\text{Ga}}T_{\text{Ga}})^2 + 16(f_{\text{As}}T_{\text{As}})^2)/|F_m|^2 \quad (6b)$$

and

$$\varphi_m = \arctan[\{(f_{\text{As}}T_{\text{As}}) + BC_{\text{imag}}\}/\{(f_{\text{Ga}}T_{\text{Ga}}) + BC_{\text{real}}\}]. \quad (6c)$$

The form factors are taken from *International Tables for Crystallography* (1995, Part C), the values for dispersion are given by Cromer & Liberman (1970) and the BC parameters are taken from Pietsch (1981). The dispersion-corrected experimental data employed in the calculation of the charge density are compiled in Table 1. They are all corrected using the same two temperature factors, shown in the last line of Table 2. The procedure to obtain B_{Ga} and B_{As} will be presented in §4.

3. Construction of experimental charge density maps

At the point **x,y,z** the valence charge density (VCD) and the difference charge density (DCD) are calculated by a Fourier summation of structure amplitude differences, ΔF

$$p(x,y,z) = 2/V \sum_{0}^{l}\sum_{-k}^{k}\sum_{-h}^{h} \Delta F(hkl) \times \exp(-2\pi i(hx + ky + lz)), \quad (7)$$

where h, k and l are the reflection indices and x, y and z are the fractional coordinates within the unit cell. ΔF are given by

$$\Delta F = |F_{\text{exp}}|\exp(i\varphi_{\text{exp}}) - |F_{\text{sph}}|\exp(i\varphi_{\text{sph}}) \quad \text{for DCD}$$
$$= |F_{\text{exp}}|\exp(i\varphi_{\text{exp}}) - |F_{\text{core}}|\exp(i\varphi_{\text{sph}}) \quad \text{for VCD.} \quad (8)$$

The $|F_{\text{exp}}|$ are the moduli of the experimental structure amplitudes corrected for anomalous dispersion, φ_{exp} are their phases taken from (4*b*), (5*c*) and (6*c*). The DCD displays the redistribution of electrons within the crystal in comparison to the model density built from free

Table 1. *Experimental structure amplitudes of various authors*

(*a*) Strong and medium intensity reflections: The extinction correction, when necessary, has been performed by the cited authors. The data are corrected for anomalous dispersion using the temperature factors given in the last line of Table 2. The first line shows the respective scale factor used for the strong and medium intensity reflections as published by: (*a*) Matsushita & Hayashi (1977); (*b*) Levalois & Allais (1986); (*c*) Kobayashi, Takama & Sato (1988); (*d*) Stevenson (1994); (*e*) Saravanan, Mohanlal & Chandrasekaran (1992); (*f*) Uno, Okano & Yukino (1970); (*g*) spherical atoms (calculated from *International Tables for Crystallography*, 1995, Vol. C). (*b*) Weak intensity reflections: The authors are those cited in the upper part of table completed by: (*h*) Pietsch (1981) and (*i*) Bilderback (1976). The structure factor phases are π, except for 222 [$\varphi = 3.36$ (*b*), (*h*), (*i*), 3.38 (*d*) and 2.85 (*e*) radian], 442 [$\varphi = 3.16$ (*d*) and 3.13 (*e*) radian] and 662 [$\varphi = 3.36$ (*e*) radian].

(*a*) Strong and medium intensity reflections

hkl	(*a*)	(*b*)	(*c*)	(*d*)	(*e*)	(*f*)	(*g*)
skal.	1.0	0.986	0.990	0.969	0.990	1.055	1.0
111	154.906	151.936	152.846	157.515	152.571	159.048	152.774
220	180.697	181.74	181.766	182.326	182.751	191.807	182.801
311	118.365	118.747	118.504	119.170	118.706	120.918	119.691
400	150.482	150.336	150.185	148.297	149.571	146.463	150.755
331	100.773	100.046	99.829	99.163	99.887	101.845	100.062
422	128.433	128.039	127.910	128.530	128.886	129.274	127.943
333	85.108	85.757	85.933	83.984	86.723	85.482	85.585
511	85.636	85.212	85.705	84.219	86.303	83.435	85.585
440	110.498	110.641	110.981	110.411	111.318	109.652	110.398
531		75.065		74.069	75.634	72.430	74.252
620		96.345	97.319	97.652	98.181	93.440	96.425
533		65.462	65.431	65.068	66.272		65.133
444	85.102	84.529	84.359	86.708	86.987		85.042
711		57.776	58.114	58.466			57.650
551			57.814	58.688			57.650

(*b*) Weak intensity reflections

hkl	(*h*)	(*b*)	(*i*)	(*d*)	(*e*)	(*f*)	(*g*)
skal.	1.0	1.0	1.0	0.969	0.573	1.055	1.0
200	6.32	6.79	6.20	6.17	5.67	5.43	5.755
222	5.64	5.35	5.67	5.23	5.38		5.381
420	6.07	6.17		6.01	6.08		6.162
600	6.64	6.48	6.52	7.28	6.13		6.544
442		6.44		6.53	6.91		6.544
622		6.30			6.48		6.330

Table 2. *Harmonic temperature factors for gallium and arsenic as published in the literature (values in parentheses are the average of B_{Ga} and B_{As})*

Author	B_{Ga} (Å^2)	$\langle B \rangle$ (Å^2)	B_{As} (Å^2)
Uno, Okano & Yukino (1971)	0.916	(0.914)	0.912
Bilderback (1976)	0.726	(0.677)	0.628
Matsushita & Hayashi (1977)		0.629	
Levalois & Allais (1986)	0.693	(0.634)	0.575
Kobayashi, Takama & Sato (1988)		0.632	
Saravanan, Mohanlal & Chandrasekaran (1992)	0.62	(0.56)	0.49
Stevenson (1994)	0.622	(0.553)	0.483
This work	0.681 (5)	(0.638)	0.594 (5)

spherical atoms. The VCD describes the same quantity relative to a structure model built by Ga^{3+} and As^{5+} independent atom cores. Thus, we calculate F_{sph} and φ_{sph} using free atomic scattering factors and F_{core} and φ_{core} from the respective core scattering factors, *i.e.* without the contribution of 4*s* and 4*p* electrons. This was carried out on the basis of the orbital scattering factors published recently by Su & Coppens (1994). The structure factor phases φ_{exp}, φ_{sph} and φ_{core} of all reflections are fairly similar except for the (111), (311) and the weak (222), (442), (622) reflections (see caption of Table 1).

At large values of $\sin\theta/\lambda$, the influence of the valence electrons on the total atomic scattering becomes negligibly small. The densities calculated by (7) converge rapidly, which is advantageous, especially in the case of a relatively limited data set. $|\Delta F|$ becomes smaller than 0.01 electrons close to $\sin\theta/\lambda \simeq 0.6$ Å^{-1} and $\sin\theta/\lambda \simeq 1$ Å^{-1} for DCD and VCD, respectively.

4. Experimental charge density maps

The DCD and VCD are calculated in the (110) plane from the six different data sets given in Table 1. The data of Matsushita & Hayashi (1977) were complemented by the five weak reflections measured by Pietsch (1981). The same data are added to those of Kobayashi, Takama & Sato (1988). Uno, Okano & Yukino's (1970) data set is used as published. For the data presented by Levalois & Allais (1986), Saravanan, Mohanlal & Chandrasekaran (1992) and Stevenson (1994), reflections out to *ca* $\sin\theta/\lambda \simeq 0.64$ Å^{-1} are employed in the synthesis of the DCD in order to obtain comparable spacial resolution and series termination errors in all cases. Although the high-order reflections should not significantly contribute to the DCD, their inclusion gives

rise to additional peaks, far away from atomic and bonding sites. This is due to the influence of a few reflections which deviate significantly from their expected value.

We have calculated all the charge densities using data which were corrected with the same two temperature factors. The reason being that the published values differ considerably (see Table 2). It follows from basic arguments that the Debye–Waller factor of an atom in a crystal is an objective quantity for describing its mean thermal displacement at a specific temperature. Therefore, there is no reason why the temperature factors should be different, performing a scattering experiment at equal temperatures. In the present case all the experiments were performed at room temperature and thus the B values should not differ. In practice, the Debye–Waller factors are used as additional refinement parameters to correct 'systematic errors' of the experiments. Another reason for disagreement is the influence of the thermal diffuse scattering which takes place when measuring integral intensities, but which is not important for dynamical diffraction experiments. Furthermore, impurities and misfit dislocations within the crystal can induce static displacements of atoms which gives rise to a static Debye–Waller factor. Static and thermal Debye–Waller factors can only be separated from each other by recording data sets at different temperatures.

However, we redetermined the temperature factors from Wilson plots. This procedure is most successful when using a data set containing a sufficient number of high-order reflections for which the influence of the valence shell on the atomic temperature factors can be neglected. For this reason the data given by Matsushita & Hayashi (1977) and Kobayashi, Takama & Sato (1988) were ruled out. For the remainder, we used the range from $|F(444)|$ up to the end of the respective data set (not all data are shown in Table 1) and a few structure factors are omitted which deviate strongly from the best straight line. Additionally, a scale factor multiplying the data was refined. The values of B_i given in the last line of Table 2 are obtained using the data from Levalois & Allais (1986). They do not differ markedly from the published values, but our slight modification changes the charge density at the atomic sites (see below). Similar procedures were performed using the data of Stevenson (1994) and Saravanan, Mohanlal & Chandrasekaran (1992). Because the fitted B_i differ considerably from the published values they were omitted from further data treatment.

For our analysis, the chosen temperature factors are assumed to be the objective values in question. They are smaller than those published by Bilderback (1975), which were applied in our previous charge density calculation (Pietsch, Tsirelson & Ozerov, 1986). The average value $\langle B \rangle$ shown in Table 2 is close to the value published by Kobayashi, Takama & Sato (1988), as well as to the average of B_{Ga} and B_{As} given by Matsushita & Hayashi (1977), but it is in total disagreement with Uno, Okano & Yukino (1970).

Table 3. *The height and the relative position of the density maxima in the calculated DCD and VCD in comparison to the respective values obtained by pseudopotential calculations and by the electron diffraction (*) maximum at the atomic sites*

Author	VCD_{max}	R_{max}	DCD_{max}
Experimental, X-ray			
Uno, Okano & Yukino (1971)	(0.91)		0.95 (0.53)
Matsushita & Hayashi (1977)	0.61	0.08	0.255
Levalois & Allais (1986)	0.62	0.002	0.260
Kobayashi, Takama & Sato (1988)	0.59	0.002	0.21
Saravanan, Mohanlal & Chandrasekaran (1992)	(0.59)		1.38 (0.09)*
Stevenson (1994)	0.76		0.36
Theory			
Walter & Cohen (1971)	0.75	0.115	
Chelikowski & Cohen (1976)	0.70	0.080	
Wang & Klein (1981)	0.75	0.173	0.125
Causà, Dovesi & Roetti (1991)	0.65	0.147	
Electron diffraction			
Zuo, Spence & O'Keefe (1988)			0.07

In the following the DCD's are calculated from the data given in Table 1. Only the maps calculated from Matsushita & Hayashi's (1977), Levalois & Allais' (1986), Kobayashi, Takama & Sato's (1988) and Stevenson's (1994) data (Figs. 1*a–d*) show a prominent charge density maximum between next neighbours. The heights of these respective charge density maxima agree fairly well (Table 3). Only Matsushita & Hayashi's (1977) data show an almost flat density outside the bonding region. Figs. 1(*b*)–(*d*) show additional density maxima, especially between second nearest neighbours. Their relative contribution to the total density can be varied by changing the scale factor. Its increase leads to a higher density close to the atomic sites and a smaller scale factor favours the density regions outside the bond, as expected. Furthermore, a slight change of the temperature factors changes the charge density close to the atomic sites. Whereas Fig. 1(*b*) displays almost equal negative values at gallium and arsenic sites, the original B values given by Levalois & Allais' (1986), fourth line of Table 2, create a much deeper charge density trough at the arsenic site than that at the gallium site, which may be misinterpreted by a larger ionicity.

The DCD calculated from Saravanan, Mohanlal & Chandrasekaran (1992), not shown, shows additional density maxima at the atomic and tetrahedral sites, which are atypical for covalently bonded materials. In Uno, Okano & Yukino's (1977) map (not shown) two subpeaks appear between next neighbours close to the atomic sites. In both cases a single maximum between next neighbours is only obtained when using the temperature factors determined by the authors themselves

(see Table 2), but the amount of the respective density maxima is much smaller (0.09 e $Å^{-3}$) or much larger (0.53 e $Å^{-3}$) than the other densities collected in Table 3.

The reason for the different shape of DCD's is explained by the graph shown in Fig. 2, which compares the $\Delta F = |F_{exp}| - |F_{sph}|$ of the first nine strong and medium intensity reflections (Fig. 2*a*) and five weak intensity reflections (Fig. 2*b*), where the $|F_{exp}|$ are given in Table 1 and the $|F_{sph}|$ are calculated with the spherical atom model. There is a typical functional shape of ΔF *versus* $h^2 + k^2 + l^2$. This is illustrated by the example of Matsushita & Hayashi's (1977) data, which give the most satisfactory density. Whereas $\Delta F(111)$ is positive, $\Delta F(220)$, $\Delta F(311)$ and $\Delta F(400)$ are negative and $\Delta F > \Delta F(331)$ becomes positive again with decreasing amount. The same functional behaviour is obtained from the other data sets, but shifted to smaller or larger *hkl*. The $\Delta F(111)$ of Levalois & Allais (1986) is negative, that of Kobayashi, Takama & Sato (1988) is close to zero *etc.* The data of Uno, Okano & Yukino (1970) do not follow such a behaviour. However, the different functional dependence of ΔF *versus hkl* results in a different charge density distribution and this explains the effect on the calculated density if scale factors are changed. Figs. 3(*a*) and (*b*) show the partial DCD calculated from the five and six weak reflections given by Pietsch (1981) and Levalois & Allais (1986), respectively (Table 1). Although the data differ slightly on the absolute scale, the partial density maps verify generally the charge density accumulation and the ionic charge transfer between next neighbours. Similar maps are obtained using the weak intensity reflections measured by Stevenson (1994) and Bilderback (1975), not shown here. The contribution of these reflections does not exceed 25% of the DCD maximum between next neighbours (0.058 and 0.055 e $Å^{-3}$, in Figs. 3*a* and *b*, respectively). On the other hand, the weak $|F|$ values from Saravanan, Mohanlal & Chandrasekaran (1992) differ by more than 100% from expectations. A scale

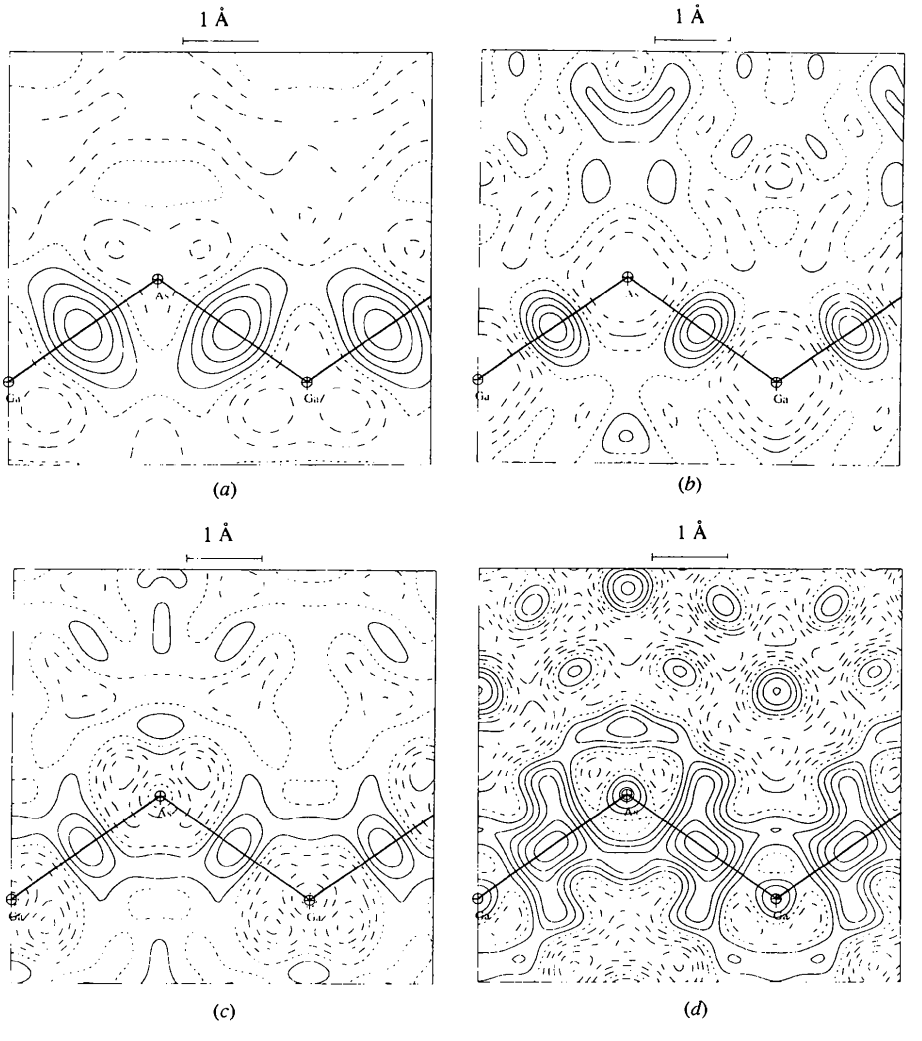

Fig. 1. DCD's calculated in the (110) plane from the data given by (*a*) Matsushita & Hayashi (1977) and Pietsch (1981), (*b*) Levalois & Allais (1986), (*c*) Kobayashi, Takama & Sato (1988) and (*d*) Stevenson (1994). The interval between the contours is 0.054 e $Å^{-3}$. Negative contours broken.

factor of *ca* 0.57 is necessary to bring these data on a similar level compared with the others. Because they also differ qualitatively, they are not used for the density calculations. Note that using only weak reflections leads to the appearance of ghost peaks in the empty space of the unit cell.

5. Comparison with theoretical density plots

Theoretical charge densities for GaAs were published by Walter & Cohen (1971), Chelikowski & Cohen (1976), Wang & Klein (1981) and Causà, Dovesi & Roetti (1991) using various pseudo-potential approaches. Outside the atomic regions they can be compared with experimental VCD maps, taking into account that the theoretical maps correspond to the static density without thermal smearing or series termination effects, whereas the experimental maps are dynamic, including these effects. Thus, the absolute peak heights of the theoretical VCD in the bonding regions are expected to be slightly larger compared with ours.

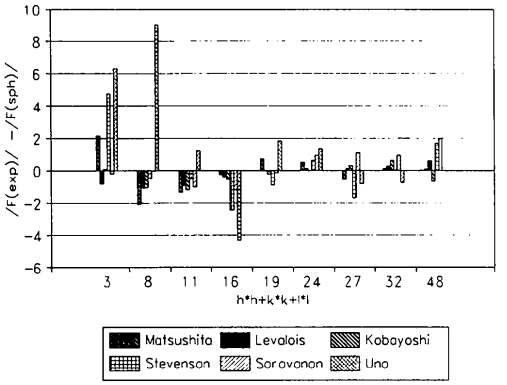

(*a*)

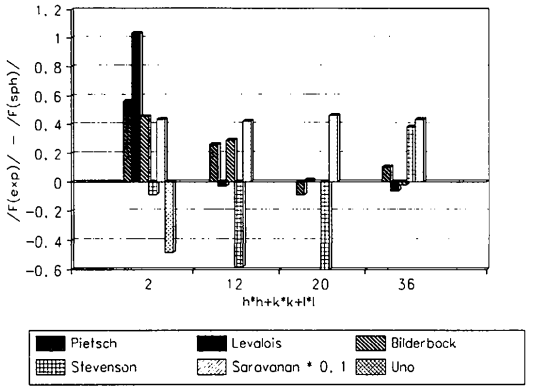

(*b*)

Fig. 2. The difference between the experimental structure amplitudes and those calculated for spherical atoms $\Delta F = |F_{exp}| - |F_{sph}|$ as a function of the square sum of Miller indices $h^2 + k^2 + l^2$ (*a*) for the first nine strong and medium intensity reflections and (*b*) for the five lowest-order weak reflections.

Fig. 4 shows the VCD calculated by Chelikowski & Cohen (1976) as a representative example. As with the other theoretical densities mentioned, it exhibits a pronounced charge density pile up between nearest neighbours shifted in the direction of the arsenic ion. This indicates the mixed covalent–ionic character of the chemical bond. No additional peaks appear outside the bond region. The VCD's calculated by Matsushita & Hayashi (1977), Pietsch (1981), see Fig. 5, Levalois & Allais (1986) and Kobayashi, Takama & Sato (1988), not shown here, are in qualitative agreement with the theoretical maps. In contrast to the pseudo-potential maps, the VCD of Levalois & Allais (1986) and Kobayashi, Takama & Sato (1988) show a higher density in the direction beyond the bond and between second next-nearest neighbours. For the other data, various disagreements appear in comparison with the theory.

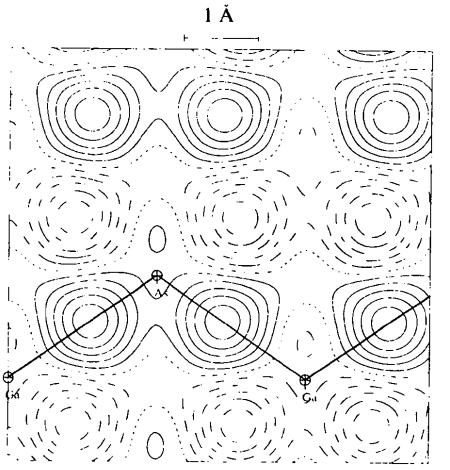

(*a*)

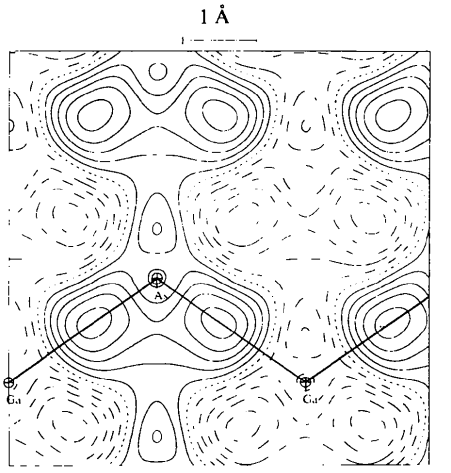

(*b*)

Fig. 3. DCD calculated from the weak intensity reflections measured by (*a*) Pietsch (1981) and (*b*) Levalois & Allais (1986). The step interval is 0.01 e Å^{-3}. Negative contours broken.

Stevenson's (1994) VCD map (not shown here) shows additional density maxima at the atomic sites and between next-nearest neighbours. The data of Saravanan, Mohanlal & Chandrasekaran (1992) and Uno, Okano & Yukino (1970) could only be used under the restrictions mentioned above. In the bonding region the density maxima are rather similar (0.59–0.62 e Å^{-3}) and are shifted slightly in the direction of the As atom. The amount of this shift ($R_{max} = r_{max} - 0.5r_{NN})/r_{NN}$ (r_{max} is the distance between the VCD maximum and the Ga atom, r_{NN} is the next-neighbour distance) differs among the various density plots. It is close to zero in the case of Levalois & Allais (1986) and Kobayashi, Takama & Sato (1988) data. In general, the pseudo-potential maps show a shift larger than zero, but also differ among the authors. As in the 'experimental' densities the amount of density at the arsenic site is larger than at the gallium site, because of the partial ionicity of the chemical bond. As expected, the experimental maps reveal a lower density maximum compared with those calculated by pseudo-potential methods (Table 3).

However, theoretical and experimental charge densities do not agree quantitatively. Although negative density regions appear outside the bond, which we explain by the influence of the limited data set, the best qualitative agreement between theory and experiment is

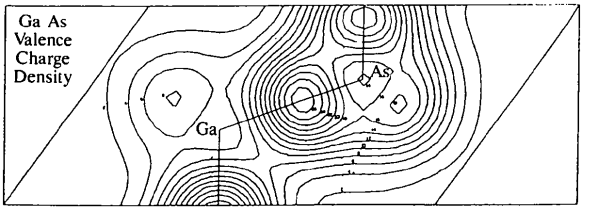

Fig. 4. VCD calculated by Chelikowski & Cohen (1976) using the pseudo-potential method. The contour interval is 0.054 e Å^{-3}.

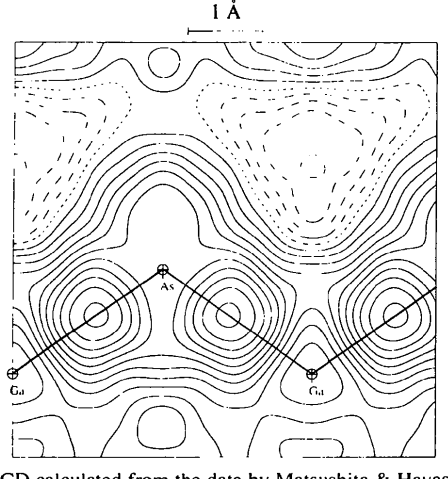

Fig. 5. VCD calculated from the data by Matsushita & Hayashi (1977) and Pietsch (1981). The contour interval is 0.054 e Å^{-3}. Negative contours broken.

obtained from the data given by Matsushita & Hayashi (1977) and Pietsch (1981), Fig. 5.

6. Discussion

Before discussing the specific results obtained for GaAs, we wish to make some general remarks.

Calculated by Fourier summation, the features of the charge density maps are very sensitive to even small errors of individual structure amplitudes. The error of a single reflection will produce spurious features in sites of high symmetry. In order to avoid this, all reflections should be measured with about the same high absolute accuracy. This is important when analysing high-symmetry materials with small unit cells. Because the number of independent reflections is small, obviously inaccurate data cannot be cancelled without the loss of information.

The influence on the features of the resulting VCD or DCD by modelling the experimental structure factor moduli may be demonstrated using, as an example, the data of Levalois & Allais (1986). After a refinement of their data, using a bond charge model, the charge density is smooth and shows no additional density maxima outside the bonding region (see Fig. 1 in Levalois & Allais, 1986). The maximum of this 'model-VCD' (0.85 e Å^{-3}) is much larger than that in our map (0.62 e Å^{-3}). The influence of an adjusted temperature factor on the density maps was already discussed in §4. Additional 'model errors' may appear if the data of this non-centrosymmetric structure are refined by a multipole expansion model (El Haouzi, Hansen, Le Henaff & Protas, 1996).

Our study shows that when working on materials with very high crystal perfection, the experiments should be performed such that the dynamical theory of X-ray diffraction is valid. This gives a unique opportunity to obtain structure amplitudes without having to correct for systematic effects such as thermal diffuse scattering contributions or secondary extinction.

In order to evaluate the uncertainty inherent in our treatment, we used two different tables of atomic scattering factors and anomalous dispersion in order to estimate their maximum influence on the corrected data and on the calculated charge density maps. The influence of the choice of different atomic scattering factors was negligible. The estimated difference between the free atomic scattering factors given in *International Tables for Crystallography* (1995, Vol. C) and the orbital scattering factors published by Su & Coppens (1994) amounts to absolute 0.1 e for $F(111)$ and 0.05 e for $F(711)$. The weak reflections are affected by almost 0.05 e for $F(200)$. This is much smaller than experimental error. A larger influence was observed using different values of anomalous dispersion. The use of either the values of Cromer & Liberman (1970) or the earlier values published affects the data of the order 1%, especially in

the case of copper radiation. This was already stated by Uno, Okano & Yukino (1970) and Kobayashi, Takama & Sato (1988). This influence becomes neglegibly small for a wavelength smaller than 0.5 Å. On the other hand, the model used for the correction of anomalous dispersion influences the calculated charge density. The application of the bond charge model, rather than the model of free atoms, changes the phases of $F(111)$, $F(222)$ and $F(311)$, but it causes only a moderate decrease of the charge maximum between next neighbours. Thus, the influence of the model is very small. A further influence may be expected taking anharmonicity into account. Its consideration requires a modification of the formalism for correcting the experimental data for anomalous dispersion (see part 2 of this work). Because the contribution of the bond charge decreases and the anharmonicity increases as a function of $\sin\theta/\lambda$, the high-order weak structure amplitudes are dominated by the anharmonicity. The strong and medium reflections are much less affected (Pietsch, 1982). We could not notice any significant change of the calculated charge densities taking anharmonicity into account. This may be due to the fact that only data with $\sin\theta/\lambda < 0.64$ Å^{-1} were used in the Fourier sum.

Qualitatively we could confirm our theoretical predictions by the experimental charge densities. Our analysis demonstrates the present state of the knowledge of the VCD of GaAs – one of the best investigated materials. The covalent–ionic character of the bond is verified by the charge density maximum between next neighbours and its shift towards the arsenic ion. This shift is more clearly observed in the VCD (compared with the DCD), because of the superposition of the 'bond charge' (overlap of bonding orbitals) and the 'spherical' valence charge close to the arsenic ion. These terms cannot be separated without additional model assumptions. Further disagreements remain outside the bonding region, especially between second nearest neighbours and in the antibonding direction. The existence of such additional density maxima cannot in general be ruled out; they could be due to electron correlation. Our calculated densities may be compared with results of other methods which are sensitive to the charge density distribution. The VCD of GaAs was studied by Zuo, Spence & O'Keefe (1988) by means of electron diffraction. Compared with the values given in Table 1, their structure amplitudes are generally too large (Table 3). Thus, the calculated DCD reproduces the covalent bond qualitatively but its maximum density is too low.

A better knowledge of the experimental charge density requires precise data for high-order reflections. They contain information about the harmonic and anharmonic lattice vibrations which are necessary in order to extract accurately the contribution of the valence charge density from the low-order reflections. A higher precision is required for strong as well as weak reflections. High-order reflections of the required accuracy have not been available until now. Therefore, a re-examination of these structure amplitudes is desirable.

This work was partially supported by the European Community under Grant ERBCHRXCT930155 in the framework of the integrated French–German collaboration (PROCOPE):DAAD (Germany) contract no. 312/pro-bmbw-gg and MAE (France) contract no. 95 111.

References

Attard, A. E. (1968). *J. Phys. D*, **1**, 390–391.
Bilderback, D. H. (1975). Thesis. Purdue University, West Lafayette, Indiana, USA.
Causà, M., Dovesi, R. & Roetti, C. (1991). *Phys. Rev. B*, **43**, 11937–11943.
Chelikowski, J. C. & Cohen, M. L. (1976). *Phys. Rev. B*, **14**, 556–582.
Cole, H. & Stemple, N. R. (1972). *J. Appl. Phys.* **33**, 2227–2233.
Colella, R. (1971). *Phys. Rev. B*, **3**, 4308–4311.
Cromer, D. T. (1965). *Acta Cryst.* **18**, 17–23.
Cromer, D. T. & Liberman, D. (1970). *J. Chem. Phys.* **53**, 1891–1898.
Dawson, B. (1967). *Proc. R. Soc. London A*, **298**, 255–263.
DeMarco, J. J. & Weiss, R. J. (1964). *Phys. Lett.* **13**, 209–210.
El Haouzi, A., Hansen, N. K., Le Henaff, C. & Protas, J. (1996). *Acta Cryst.* A**52**, 291–301.
Hansen, N. K. & Coppens, P. (1978). *Acta Cryst.* A**34**, 909–921.
Kobayashi, K., Takama, T. & Sato, S. (1988). *Jpn. J. Appl. Phys.* **27**, 1377–1380.
Levalois, M. & Allais, G. (1986). *Acta Cryst.* B**42**, 442–449.
Matsushita, T. & Hayashi, J. (1977). *Phys. Status Solidi A*, **41**, 139–145.
Pietsch, U. (1981). *Phys. Status Solidi B*, **103**, 93–100.
Pietsch, U. (1982). *Phys. Status Solidi B*, **111**, 9–12.
Pietsch, U., Paschke, K. & Eichhorn, K. (1993). *Acta Cryst.* B**49**, 822–825.
Pietsch, U., Paschke, K. & Eichhorn, K. (1994). *Acta Cryst.* B**50**, 780.
Pietsch, U., Tsirelson, V. G. & Ozerov, R. P. (1986). *Phys. Status Solidi B*, **138**, 47–52.
Roberto, J. B., Batterman, B. W. & Keating, D. (1974). *Phys. Rev. B*, **9**, 2590–2599.
Saravanan, R., Mohanlal, S. K. & Chandrasekaran, K. S. (1992). *Acta Cryst.* A**48**, 4–9.
Stevenson, A. W. (1994). *Acta Cryst.* A**50**, 621–632.
Stewart, R. F. (1976). *Acta Cryst.* A**32**, 565–574.
Su, Z. & Coppens, P. (1994). Sagamore XI. International Conference on Charge, Spin and Momentum Densities, 7–12 August 1994. Brest, France.
Uno, R., Okano, T. & Yukino, K. (1970). *J. Phys. Soc. Jpn*, **28**, 437–442.
Walter, J. P. & Cohen, M. L. (1971). *Phys. Rev. B*, **4**, 1877–1892.
Wang, C. S. & Klein, B. M. (1981). *Phys. Rev. B*, **24**, 3393–3416.
Willis, B. T. M. & Pryor, A. W. (1975). *Thermal Vibrations in Crystallography*. Cambridge University Press.
Zuo, J. M., Spence, J. C. & O'Keefe, M. (1988). *Phys. Rev. Lett.* **61**, 353–356.